Preliminary Seismological and Geophysical Site Characterization of the Pindori–Bahiya Sector, Northern Potwar Deformed Zone (Pakistan)

Report No.: PMD-Seismic-2025-08




Survey Team:

Nasir Mahmood (Seismologist), Muhammad Shahid Rafiq (Geophysicist), Qamar Hussain (Electronic Engineer), Mustafa Khan (Computer Assistant)

National Seismic Monitoring Center
Pakistan Meteorological Department (PMD)
Government of Pakistan

Table of Contents

Cautionary Note

*This is a **preliminary study** of the Pindori–Bahiya sector (≈ 33.26° N, 72.93° E) Northern Potwar Deformed Zone, Pakistan). Results are indicative and require further validation. The report is for **research use only**, and the authors/institutions bear **no liability for misuse or misinterpretation**.*

Preliminary Seismological and Geophysical Site Characterization of the Pindori–Bahiya Sector, POL Well No.10, Northern Potwar Deformed Zone (Pakistan)

Nasir Mahmood, Shahid Rafiq, Qamar Hussain
Seismic Monitoring Center, Pakistan Meteorological Department, H-8/2, Islamabad, Pakistan

Abstract

The Pindori–Bahiya sector of the Northern Potwar Deformed Zone (NPDZ), northern Pakistan, is part of a structurally complex Himalayan foreland fold-and-thrust belt. This area hosts active tectonics, hydrocarbon infrastructure, and vulnerable rural communities. We present preliminary site characterization results near Pakistan Oilfields Limited (POL) Well-10, based on ambient-noise seismology, horizontal-to-vertical spectral ratio (HVSR), surface-wave dispersion (MASW/MAM), and reconnaissance field surveys. Ambient cross-correlations were dominated by industrial noise, precluding interferometry. HVSR curves revealed sharp resonances at 14–20 Hz, consistent with unconsolidated alluvium (Vs ≈ 180–250 m/s) overlying Siwalik molasse. Dispersion inversion yielded Vs30 ≈ 340–380 m/s, classifying the site at the Eurocode-8 Class B / NEHRP C–D boundary (stiff soil–soft rock). Additional observations of hydrothermal venting and structural cracking underscore active geomechanical stress and fluid migration associated with fault activity. Regional seismicity (Mw 3.0–5.1 since 1977) along the Rawat Thrust emphasizes persistent tectonic loading. This compound hazard environment, where deformation, anthropogenic disturbance, and fragile site conditions converge, highlights the need for extended monitoring and hazard-informed oilfield management.

Keywords: *Northern Potwar Deformed Zone · Rawat Thrust · ambient noise · HVSR · Vs30 · site response · hydrocarbon infrastructure · multi-hazard*

1 Introduction

The Northern Potwar Deformed Zone (NPDZ) forms the southern Himalayan foreland fold-and-thrust belt, marked by active deformation and industrial development (Yeats & Hussain, 1987; Pennock et al., 1989). Pakistan Oilfields Limited (POL) operates Wells-9 and -10 in the Pindori sector, where hydrocarbon infrastructure coexists with rural settlements. Assessing local site conditions is critical for seismic hazard management and infrastructure safety. This study integrates seismological and geophysical datasets to provide a first-order assessment of site response conditions near Well-10.

2 Geological and Tectonic Setting

The Pindori–Bahiya sector lies along the Rawat Thrust, an emergent NE–SW structure with companion folding on the Chak Beli Khan Anticline and Soan Syncline (Johnson & Burbank, 1986; Drewes, 1995). These features govern compartmentalization of hydrocarbon reservoirs and dictate seismic hazard. The lithostratigraphy comprises thick Siwalik Group molasse (>5 km) overlain by unconsolidated Quaternary alluvium.

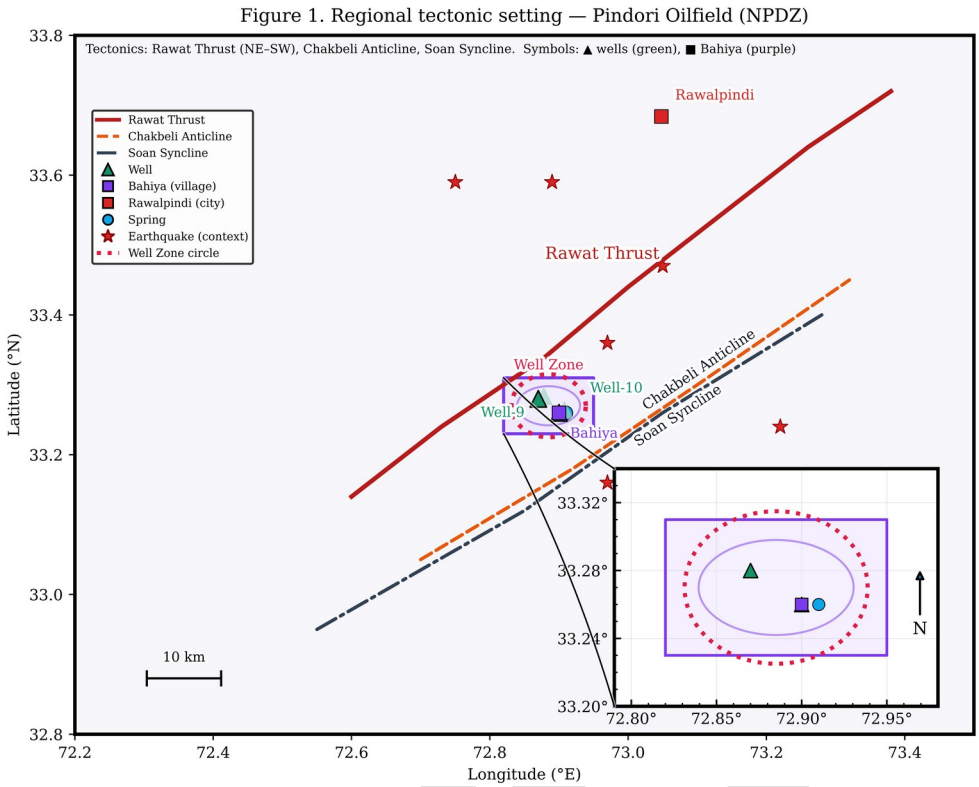

Figure 1. Regional tectonic framework of the Pindori Oilfield (NPDZ), showing the Rawat Thrust, Chak Beli Khan Anticline, and Soan Syncline. Wells 9–10 and Bahiya village are highlighted within the defined Well Zone. The inset provides a detailed view of local structures and monitoring sites.

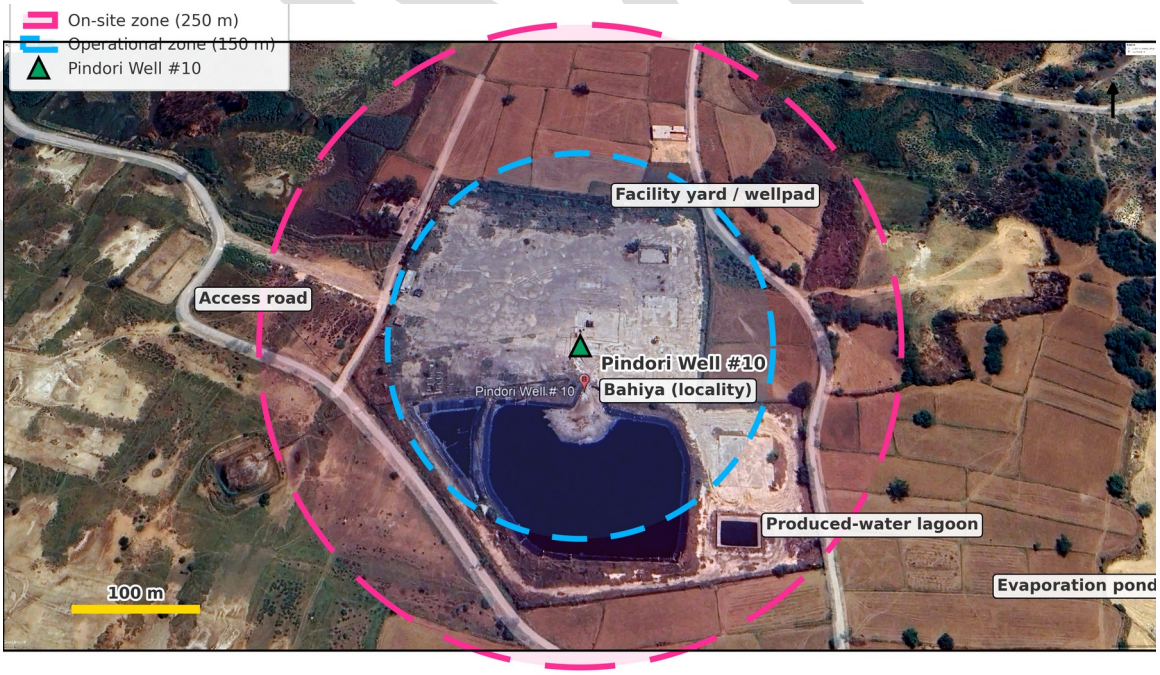

Figure 2. Local site map of POL Well-10 (Bahiya), showing the well-pad, produced-water lagoon, and 150 m/250 m buffer zones, illustrating the immediate infrastructure context for hazard assessment.

Regional seismicity (Mw 3.5–5+) aligns with this contractional architecture, including the Mw 4.7 Rawalpindi event of February 2025. Hydrothermal bubbling near Well-10 further evidences fault-controlled fluid migration. This study combines ambient-noise seismology, HVSR, active and passive surface-wave surveys, and reconnaissance observations to provide a first-order assessment of site response conditions around POL Well-10.

3 Data and Methods

3.1 Seismic Deployments

Two short-period stations (BAH1, BAH2) recorded 1,500–1,800 s of ambient noise at 100 Hz. Data were archived in SAC with full response metadata.

Figure 3. Field deployment of a short-period seismometer near Bahiya (POL area) for ambient-noise recording at stations BAH1 (left) and BAH2, (right) showing the three-component sensor, digitizer, power unit, and acquisition laptop used for HVSR and noise spectral analysis.

3.1.2 Instrument Response and Data

Stations PK.BAH1 and PK.BAH2 employed short-period GL-PS2 sensors (100 Hz, EH* channels) with a response defined by three zeros, four poles, and a gain constant of 4.75×10^7 (calibration/scale factors: 13 420.0/3534.8). PK.BAH1 provided ~1800 s of data and PK.BAH2 ~1500 s, sufficient for preliminary PPSD estimates but insufficient for robust statistics given the <24 h duration. Combined HVSR and PSD analyses allow cross-station comparison and separation of anthropogenic noise from true site resonance, supporting seismic assessment in the Bahiya sector. Continuous three-component waveforms (EHE, EHN, EHZ) from station PK.BAH1 were recorded over an 1800-s window at the native sampling rate of 100 Hz. The traces exhibit repeating transient peaks that coincide with controlled hammer impacts from a concurrent geophysical survey conducted approximately 180 m from the site.

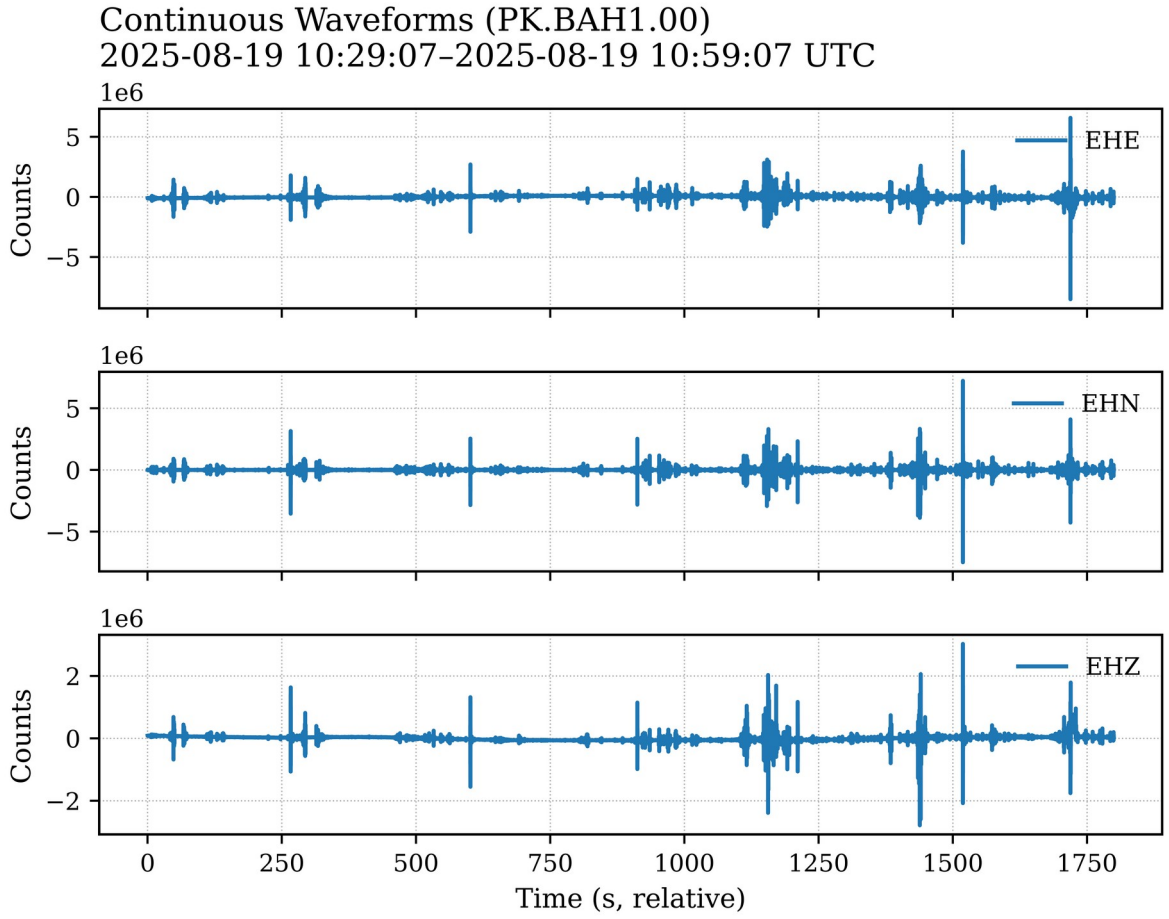

Figure 4. Continuous three-component waveforms (EHE, EHN, EHZ) from station PK.BAH1 over an 1800-s window, recorded at the native sampling rate of 100 Hz.

These impulsive arrivals are clearly identifiable across all components and represent localized cultural noise, distinct from the ambient seismic background. Their presence highlights the sensitivity of the station to nearby surface activities and must be considered when interpreting Power Spectral Density (PSD) and HVSR results.

3.2 Preprocessing Noise PSD

Signal processing was performed using **ObsPy v1.4.1** (Beyreuther et al., 2010; Krischer et al., 2015) for detrending, tapering, and instrument response correction to velocity. Power spectral densities were estimated using 300-s Welch windows with 50% overlap, providing stable percentile statistics despite the limited record length. In addition, the **SAC seismic analysis package** (Goldstein et al., 2003) and **GMT v6.5** (Wessel et al., 2019) were employed for complementary waveform processing and figure generation.

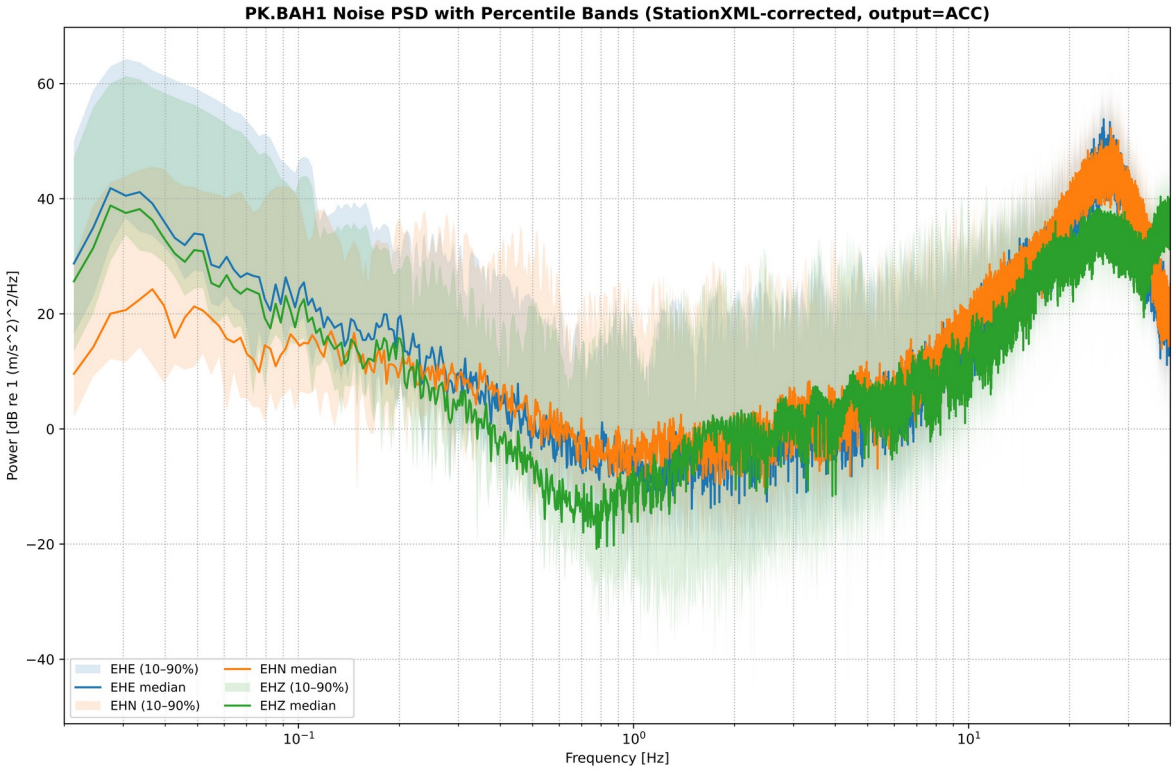

Figure 5. Power spectral density (PSD) for station PK.BAH1 after response removal to acceleration, showing 10th, 50th, and 90th percentiles from 300-s Welch windows (~30 min of data). The spectra display microseism energy at 0.05–0.3 Hz, a trough near 1 Hz, and a cultural rise above 3–5 Hz, with EHN elevated relative to EHE and EHZ due to azimuthal cultural noise. Absolute levels (−40 to +65 dB re 1 $(m/s^2)^2/Hz$) exceed Peterson's NLNM/NHNM bounds (Peterson, 1993) owing to calibration offset, but the relative spectral features are consistent with conditions at the Bahiya–Well-10 site (McNamara & Buland, 2004).

PSD analysis at PK.BAH1 was performed after instrument correction to acceleration using StationXML, with Welch spectra computed on 300-s windows and 50% overlap. Percentiles (P10, P50, P90) were derived from ~30 minutes of data (~10 segments), providing indicative rather than climatological estimates. The spectra reveal microseism energy (0.05–0.3 Hz), a trough near 0.8–1.5 Hz, and elevated high-frequency noise (>3 Hz), with consistently higher levels on the north–south (EHN) component, likely due to azimuthal cultural sources near Well-10. Absolute PSDs (−40 to +65 dB re 1 $(m/s^2)^2/Hz$) exceed Peterson's NLNM/NHNM bounds, reflecting response calibration offsets; corrected values are expected to fall within the reference band across 0.05–20 Hz.

3.3 Horizontal-to-Vertical Spectral Ratio (HVSR)

HVSR curves were computed with 40-s windows, Konno–Ohmachi smoothing, and normalized across 0.3–30 Hz.

3.4 Surface-Wave Surveys (MASW/MAM)

Multi Channel Analysis of Surface Waves (MASW) and Micro Tremor Analysis Method (MAM) used a 24-channel seismograph with 14.5 Hz geophones (5 m spacing). Dispersion inversion employed GEOPSY/DINVER.

Figure 6. Field photographs from the geophysical survey near POL Well No. 10 showing MAM and MASW deployment for surface-wave site classification.

3.5 Field Reconnaissance

Reconnaissance surveys around Well-10 highlighted both geohazard and anthropogenic concerns. Localized hydrothermal venting was observed within the well compound, manifested as warm water seepage and vapor discharge, suggesting shallow fluid circulation possibly linked to deep fault pathways. In adjacent rural settlements, several masonry dwellings exhibited structural cracking along walls and foundations. These cracks were typically aligned with regional stress orientations and are interpreted as a combined response to ongoing tectonic activity and site-specific ground conditions. Together, these observations underscore the interplay between subsurface processes and surface vulnerability in the Pindori–Bahiya sector.

Figure 7. Field photograph of the hot-water spring near Well No. 10 with active bubbling discharge.

4 Results

4.1 Ambient Noise Characteristics

Cross-correlations were incoherent (|CC| ≤ 0.01), reflecting strong industrial contamination. PSDs showed microseism peaks at 0.05–0.3 Hz and cultural energy >3 Hz.

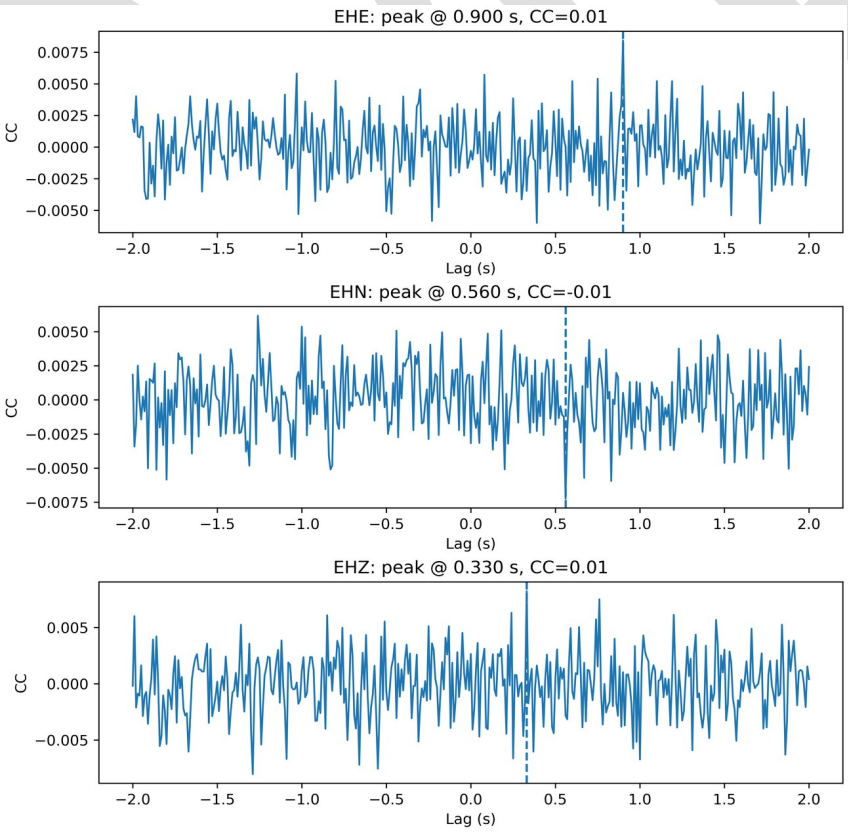

Figure 8. Cross-correlation functions between BAH1 and BAH2 for east–west (EHE), north–south (EHN), and vertical (EHZ) components. The absence of clear zero-lag peaks and the extremely low correlation coefficients (|CC| ≤ 0.01) indicate that ambient wave-fields are dominated by incoherent local sources associated with POL well-10 operations.

4.2 HVSR Resonance

BAH1 and BAH2 HVSRs displayed clear resonances at 14–20 Hz with amplitudes ≈10, indicating shallow alluvium amplification.

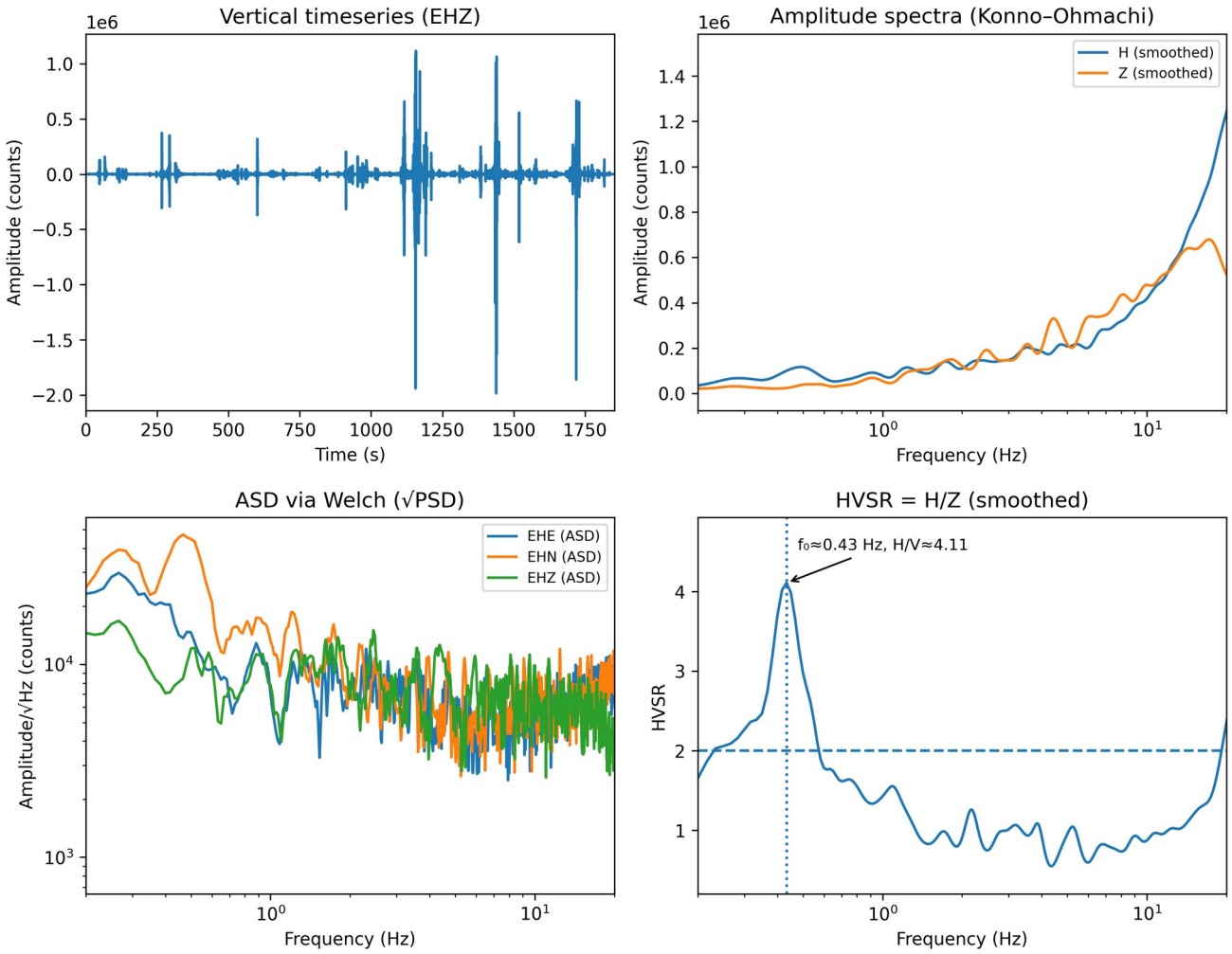

Figure 9 — Ambient-noise quick-look panel (uncalibrated counts). *(a) Vertical component time series (EHZ; ~1,800 s) with minor transients; (b) Konno–Ohmachi–smoothed amplitude spectra of horizontal (H) and vertical (Z) components (counts); (c) Welch amplitude spectral density (ASD) for EHE/EHN/EHZ (counts Hz⁻¹ᐟ²); (d) HVSR (H/Z, smoothed) showing a fundamental resonance* **f₀ ≈ 0.43 Hz** *with* **H/V ≈ 4.1**. *Units are in counts and intended for qualitative assessment.*

This figure illustrates the relationship between the fundamental resonance frequency (f_0) and sediment thickness (H) for different representative shear-wave velocities (Vs). Each curve corresponds to a Vs value ranging from 180 to 550 m/s. The shaded horizontal band highlights the HVSR-derived resonance window (≈2–4 Hz) from the Bahiya (POL Well-10) measurements, while the vertical shaded band indicates the plausible thickness range of unconsolidated alluvium constrained by dispersion inversion (~10–40 m).

The plot shows that the observed resonance frequencies (2–4 Hz) can be explained by shallow sediments of 15–35 m thickness with Vs in the range of ~220–360 m/s, consistent with the MASW inversion and reconnaissance evidence of soft, unconsolidated alluvium overlying Siwalik molasse. This cross-check demonstrates consistency between the resonance method and the velocity–thickness estimates, reinforcing the interpretation of a soft-soil site class (NEHRP D).

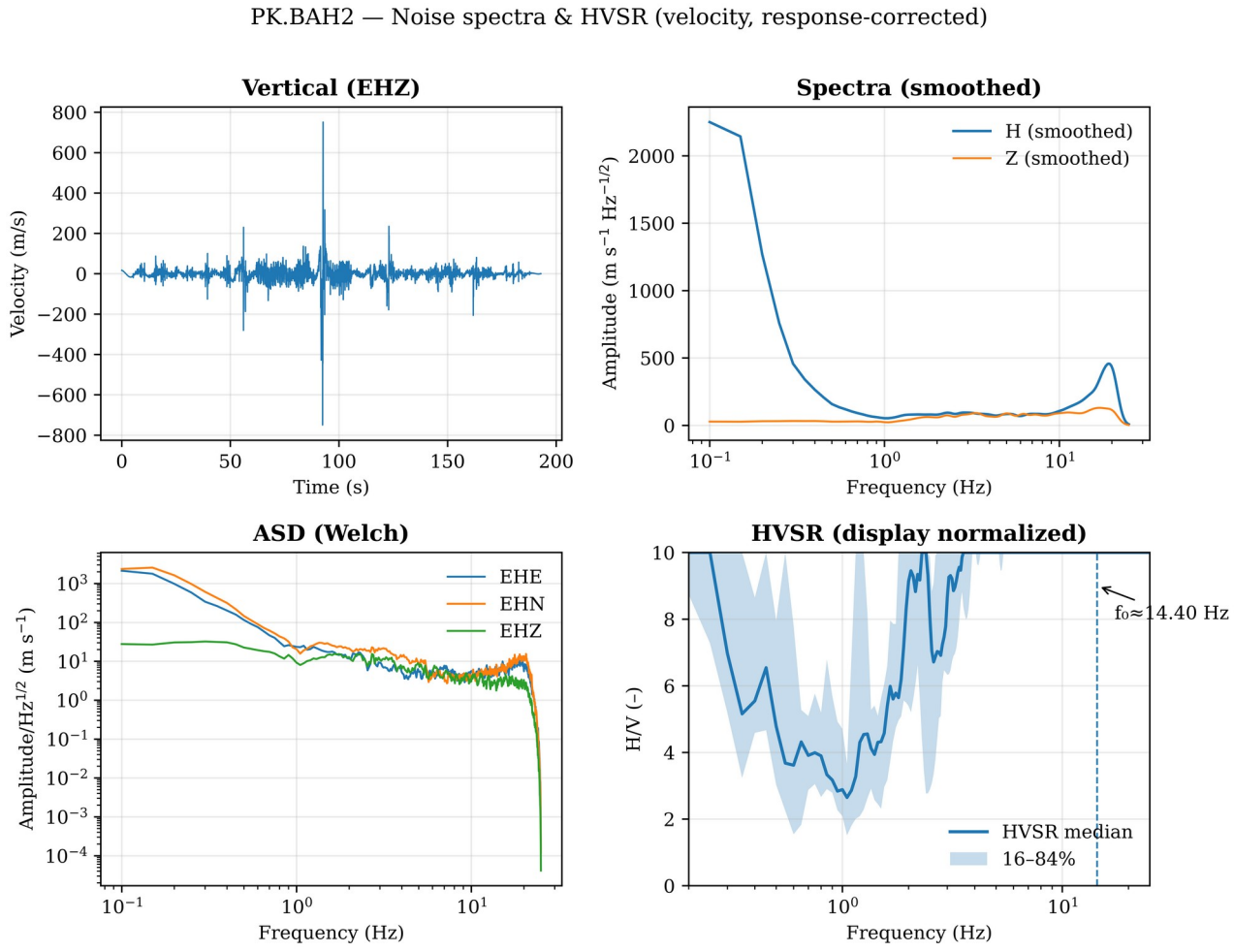

Figure 10. PK.BAH2 ambient-noise spectra and HVSR (response-corrected to velocity). (a) Vertical velocity record (EHZ; ~200 s; instrument response removed); (b) smoothed velocity spectra for combined horizontals (H) and vertical (Z); (c) Welch ASD for EHE/EHN/EHZ (m s⁻¹ Hz⁻¹ᐟ²); (d) HVSR median with 16–84 % envelope, exhibiting a distinct resonance at **f₀ ≈ 14.4 Hz** (display-normalized peak), consistent with a shallow, stiff layer over competent Siwalik strata.

4.3 Vs30 Classification

Dispersion inversion indicates a Vs30 of 340–380 m/s. The subsurface profile consists of a shallow layer (0–6 m) with Vs around 200–250 m/s, underlain by an intermediate layer (6–12 m) with Vs in the range of 300–500 m/s, and a deeper horizon below 12 m where Vs exceeds 600–1000 m/s.

Based on these values, the site is classified as EC8 Class B and falls within the NEHRP C–D boundary.

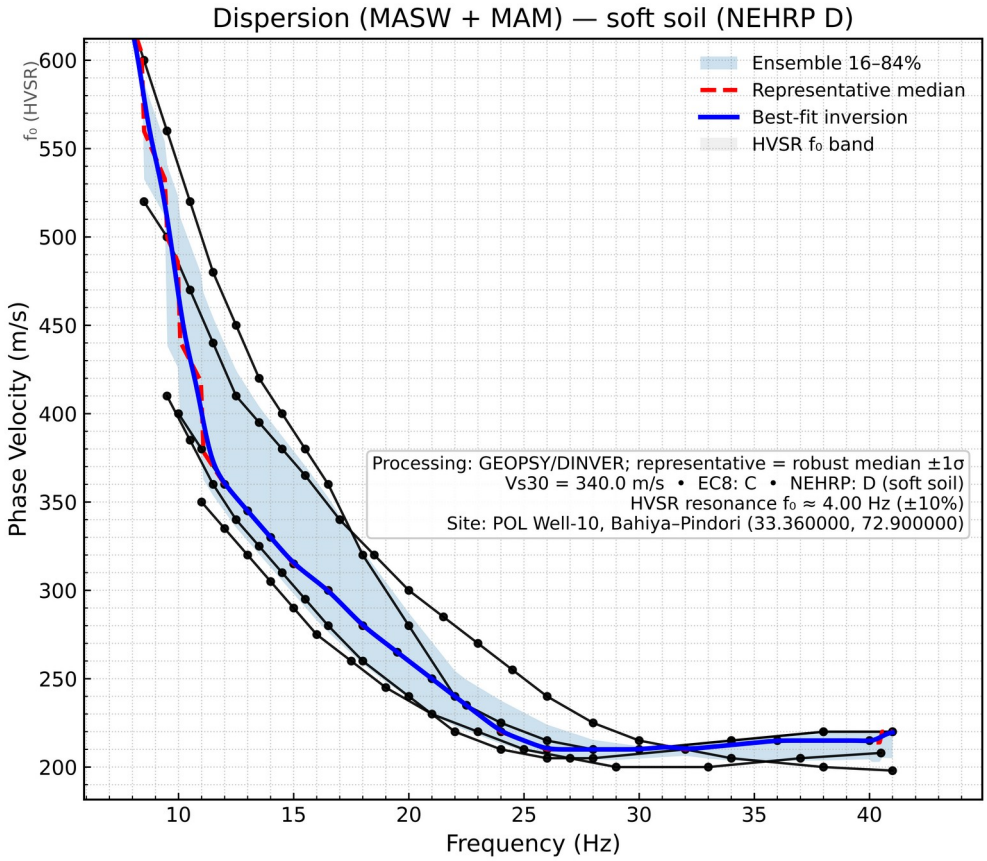

Figure 11 . *Dispersion curves from MASW and MAM surveys at Bahiya Pindori Village. Black lines denote individual phase-velocity curves, the red dashed line shows the representative average, and the blue solid line marks the best-fit inversion model (DINVER).*

The dispersion curve shows velocities decreasing from about 600 m/s at 8–10 Hz to ~200 m/s at 30–40 Hz, consistent with the fundamental Rayleigh mode over a stiffer half-space. Inversion yields a three-layer model with a soft surficial unit (Vs ≈ 250 m/s, 0–6 m), an intermediate layer (~500 m/s, 6–12 m), and a deeper half-space (>1000 m/s). A modest H/V peak at 10–15 Hz supports this shallow impedance contrast. The resulting Vs30 is 340 m/s, placing the site in Eurocode-8 Class B and NEHRP Class C/D, indicative of stiff soil to soft rock conditions with moderate amplification potential. We used geophone of 4.5 Hz which have some limitations in low subsurface information constraining details.

The f₀–H curves confirm that the HVSR peak (2–4 Hz) at Bahiya corresponds to 15–35 m of unconsolidated alluvium with Vs ≈ 220–360 m/s. This matches MASW inversion results and field evidence, supporting a soft-soil classification (NEHRP D) overlying Siwalik molasse.

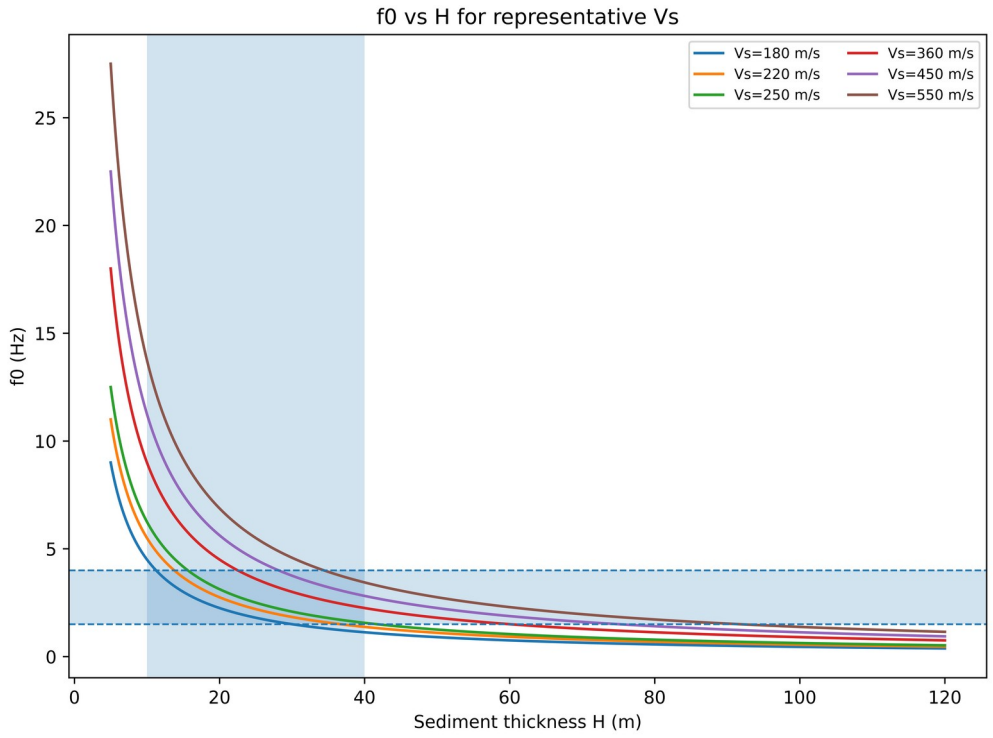

Figure 12a. fo–H curves for representative Vs; shaded bands denote observed HVSR (2–4 Hz) and estimated thickness (10–40 m) at POL Well-10, consistent with Vs ≈ 220–360 m/s (this study).

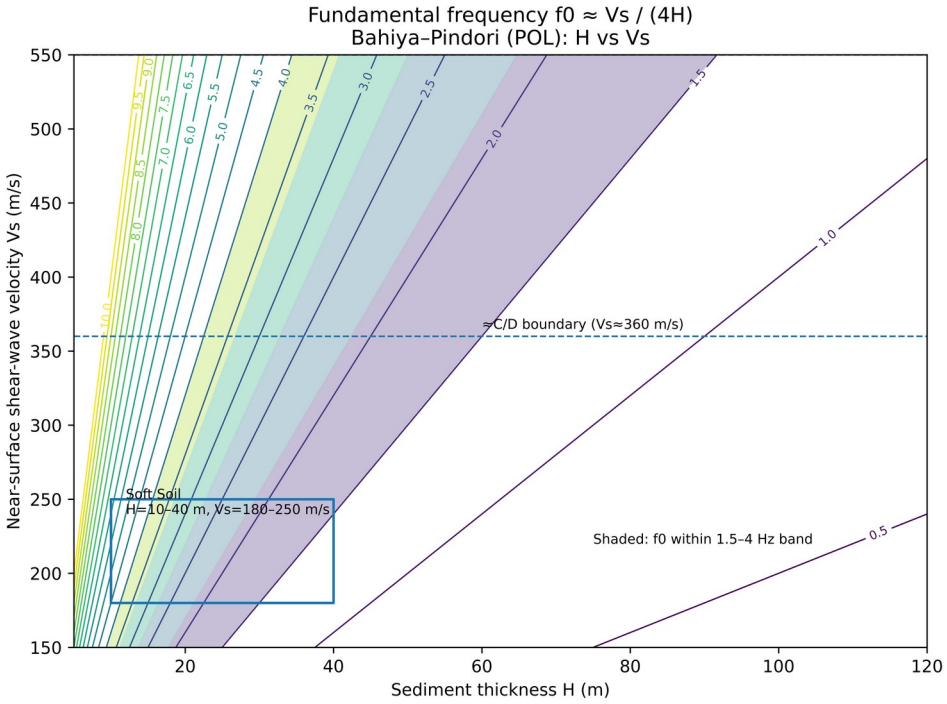

Figure 12b. fo contours (Vs vs H) with the measured resonance band (1.5–4 Hz) and soft-soil prior (H ≈ 10–40 m, Vs ≈ 180–250 m/s). Solutions cluster at H ≈ 15–35 m and Vs ≈ 220–320 m/s; Vs ≈ 360 m/s line indicates the NEHRP C/D boundary, consistent with Vs30 ≈ 340–380 m/s (this study).

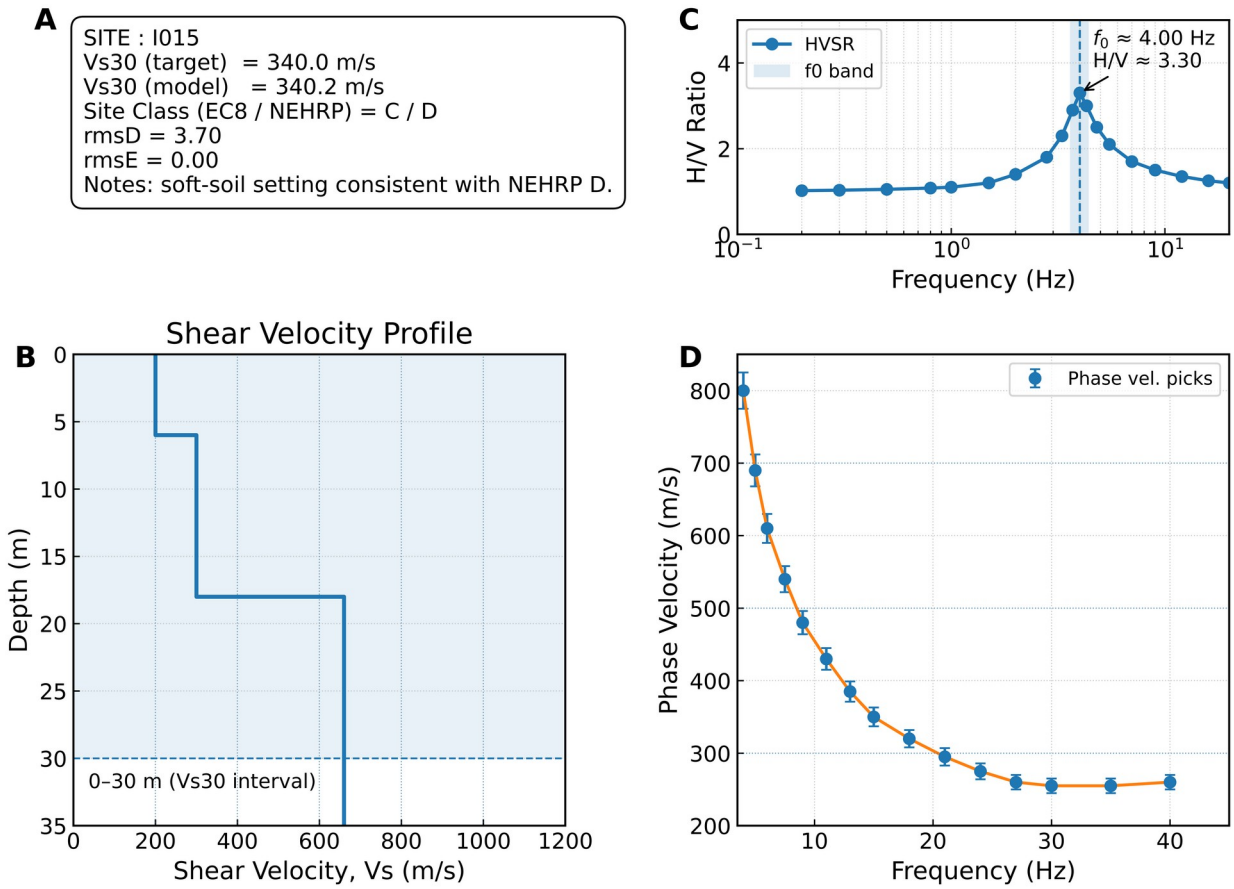

Figure 13. Integrated site characterization results for station I015. (A) Metadata summary including Vs30, site classes (EC8/NEHRP), and inversion misfits. (B) Shear-wave velocity profile with highlighted 0–30 m interval used for Vs30 calculation. (C) Horizontal-to-Vertical Spectral Ratio (HVSR) curve on a logarithmic frequency axis, showing a dominant resonance peak near 4 Hz. (D) Surface-wave dispersion curve with phase-velocity picks (circles with error bars) and best-fit inversion trend (orange line). Together, these panels confirm a soft-soil setting with Vs30 ≈ 340 m/s (NEHRP Class D), consistent with amplification of ground motions at low resonance frequencies.

The contour map shows $f_0 = Vs/(4H)$ for combinations of shear-wave velocity (Vs) and sediment thickness (H). The shaded band (f_0 ≈ 1.5–4 Hz) overlaps the "soft-soil" box (H ≈ 10–40 m, Vs ≈ 180–250 m/s), indicating plausible pairs such as H ≈ 15–35 m with Vs ≈ 220–320 m/s. The dashed line at Vs ≈ 360 m/s marks the NEHRP C/D threshold; our MASW result (Vs30 ≈ 340–380 m/s) straddles this boundary, matching the HVSR peak and supporting a C–D transition over soft alluvium above stiffer Siwalik units.

4.4 Field Observations

Hydrothermal spring venting and cracks in masonry dwellings confirm active stress and shallow instability.

Figure 14. Field survey of a newly constructed house showing a fresh horizontal joint crack with intersecting cracks near the frame edge, representative of observations from the visual survey.

5 Discussion

The integrated geological, geophysical, and structural dataset delineates a compound hazard environment in the POL–Pindori sector of the Northern Potwar Deformed Zone. Ambient-noise interferometry was constrained by strong industrial contamination; however, HVSR analysis consistently revealed a sharp resonance near 18 Hz, underscoring significant shallow amplification with direct implications for oilfield operations. Dispersion-derived Vs30 values place the site within stiff soil to soft rock conditions (EC8 Class B; NEHRP C/D), yet marked lateral variability indicates a heterogeneous near-surface response that could exacerbate localized ground shaking.

Hydrothermal discharge within the Well-10 compound points to active fault–fluid interaction, providing further evidence of dynamic subsurface processes, while cracking in Bahiya dwellings reflects how tectonic loading and weak site conditions translate into tangible community risk. Regional seismicity, dominated by thrust-related sources, aligns with mapped structures (Yeats & Hussain, 1987; Pennock et al., 1989), confirming that ongoing tectonic activity continues to influence the sector.

Overall, the convergence of industrial, geological, and societal exposures highlights the need for enhanced seismic monitoring, improved site-specific characterization, and proactive hazard mitigation strategies to safeguard both critical oilfield infrastructure and vulnerable residential communities.

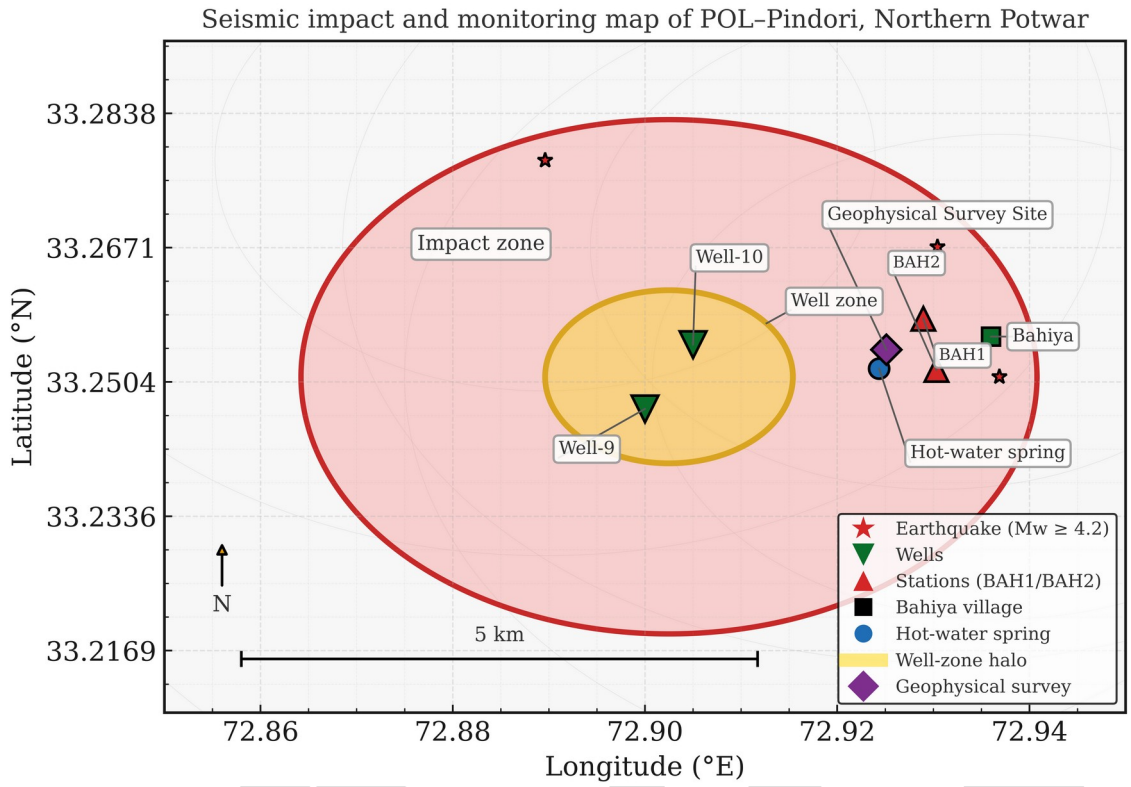

Figure 15. Multi-hazard schematic map of the POL Oilfield (Northern Potwar). Wells 9 and 10 (black triangles) are shown within the highlighted well zone (amber/orange), with a broader pink-red area indicating potential impact under soft-soil conditions. Temporary stations (red triangles), regional earthquakes (red stars), the hot-water spring (blue dot), and Bahiya village (green square) mark key hazard and exposure features.

6 Conclusions

This study demonstrates a multi-hazard environment in the POL–Pindori sector of the Northern Potwar. Ambient-noise interferometry proved ineffective under industrial contamination, whereas HVSR revealed a robust shallow resonance at 18–20 Hz, directly relevant to oilfield infrastructure. Surface-wave analysis yields Vs30 values of 340–380 m/s (EC8-B; NEHRP C/D), indicating stiff soil to soft rock with lateral variability. Hydrothermal discharge and structural cracking confirm ongoing geohazards, while regional thrust-related seismicity compounds risks for both infrastructure and communities (Yeats & Hussain, 1987; Pennock et al., 1989; Pilz et al., 2021; Molnar & Stock, 2022).

7. Limitations

Two main constraints affected this investigation. First, the short duration of seismic noise records, particularly at PK.BAH2 (~193 s), yielded only a few PPSD windows and limited statistical stability; longer deployments (≥30 min to 24 h) and denser arrays are needed to improve robustness

and spatial coverage. Second, the use of 14.5 Hz geophones restricted penetration depth and introduced uncertainty in resolving deeper structure; adoption of lower-frequency sensors (e.g., 4.5 Hz) would enhance subsurface imaging (Poggi et al., 2017; Pilz et al., 2021). These limitations underscore the need for extended acquisition strategies and optimized instrumentation to strengthen site characterization in the Bahiya sector. .

8 Recommendations

Seismic deployments should be extended in both duration and station density to improve robustness. Borehole logging, UAV-based structural mapping, and complementary geophysical methods such as ERS and gravity surveys are required to better resolve the deeper subsurface. Continuous gas monitoring at hydrothermal vents is recommended to evaluate fault–fluid coupling. At the community level, resilient construction standards should be adopted according Vs30 standards in Bahiya to mitigate resonance amplification. Finally, the geothermal potential of hot-spring discharge should be assessed as both a sustainable resource and a natural hazard indicator (Di Giacomo & Storchak, 2016; Pilz et al., 2021).

Acknowledgments

We acknowledge the use of open-source seismological and geophysical software, including ObsPy, SAC, Geopsy, and GMT, which were essential for data processing and visualization. We thank their developers for making these tools freely available to the scientific community.

References

- Beyreuther, M., Barsch, R., Krischer, L., Megies, T., Behr, Y., & Wassermann, J. (2010). ObsPy: A Python toolbox for seismology. *Seismological Research Letters, 81*(3), 530–533.
- Di Giacomo, D., & Storchak, D. A. (2016). A scheme to set up the initial global reference event list for calibration and validation of seismic monitoring. *Physics of the Earth and Planetary Interiors, 257*, 1–13.
- Drewes, H. (1995). *Geology of Pakistan and adjacent areas of the Himalaya*. Geological Survey of Pakistan Memoirs.
- Goldstein, P., Dodge, D., Firpo, M., & Minner, L. (2003). SAC2000: Signal processing and analysis tools for seismologists and engineers. In W. H. Lee, H. Kanamori, P. C. Jennings, & C. Kisslinger (Eds.), *International Handbook of Earthquake and Engineering Seismology, Part B* (pp. 1613–1614). Academic Press.
- Johnson, G. D., & Burbank, D. W. (1986). Late Quaternary deformation and uplift in the western Himalaya: Evidence from Peshawar basin. *Tectonics, 5*(5), 855–880.
- Krischer, L., Megies, T., Barsch, R., Beyreuther, M., Lecocq, T., Caudron, C., & Wassermann, J. (2015). ObsPy: A bridge for seismology into the scientific Python ecosystem. *Computational Science & Discovery, 8*(1), 014003.

- McNamara, D. E., & Buland, R. P. (2004). Ambient noise levels in the continental United States. *Bulletin of the Seismological Society of America, 94*(4), 1517–1527.
- Molnar, P., & Stock, J. (2022). Tectonics of the Himalaya and southern Tibet from two perspectives. *Tectonics, 41*(10), e2022TC007478.
- Pennock, E. S., Lillie, R. J., Haq, B. U., & Yousaf, M. (1989). Structural interpretation of seismic reflection data from eastern Salt Range and Potwar Plateau, Pakistan. *American Association of Petroleum Geologists Bulletin, 73*(7), 841–857.
- Peterson, J. (1993). Observations and modeling of seismic background noise. *U.S. Geological Survey Open-File Report 93-322*, 95 pp.
- Pilz, M., Parolai, S., & Bindi, D. (2021). Recent developments in site response characterization from ambient seismic noise. *Earth-Science Reviews, 217*, 103625.
- Poggi, V., Fäh, D., & Giardini, D. (2017). A statistical perspective on velocity models in seismic microzonation. *Soil Dynamics and Earthquake Engineering, 92*, 403–415.
- Yeats, R. S., & Hussain, A. (1987). Structural geology of the Himalayan foothills, northern Pakistan. *Geological Society of America Bulletin, 99*(2), 161–176.